

Limiting Ionic Conductance of Symmetrical, Rigid Ions in Aqueous Solutions: Temperature Dependence and Solvent Isotope Effects

Ranjit Biswas and Biman Bagchi*[‡]

Contribution from the Solid State and Structural Chemistry Unit, Indian Institute of Science, Bangalore 560 012, India

Received January 15, 1997. Revised Manuscript Received April 11, 1997[⊗]

Abstract: Limiting ionic conductance (Λ_0) of rigid symmetrical unipositive ions in aqueous solution shows a strong temperature dependence. For example, Λ_0 more than doubles when the temperature is increased from 283 to 318 K. A marked variation also occurs when the solvent is changed from ordinary water (H_2O) to heavy water (D_2O). In addition, Λ_0 shows a nonmonotonic size dependence with a skewed maximum near Cs^+ . Although these important results have been known for a long time, no satisfactory theoretical explanation exists for these results. In this article we present a simple molecular theory which provides a nearly quantitative explanation in terms of microscopic structure and dynamics of the solvent. A notable feature of this theory is that it does not invoke any nonquantifiable models involving *solvent-berg* or *clathrates*. We find the strong temperature dependence of Λ_0 to arise from a rather large number of microscopic factors, each providing a small but nontrivial contribution, but all acting surprisingly in the same direction. This work, we believe, provides, for the first time, a satisfactory explanation of both the anomalous size and temperature dependencies of Λ_0 of unipositive ions in molecular terms. The marked change in Λ_0 as the solvent is changed from H_2O to D_2O is found to arise partly from a change in the dielectric relaxation and partly from a change in the effective interaction of the ion with the solvent.

I. Introduction

Limiting ionic conductance (Λ_0) of small rigid symmetrical ions in common dipolar solvents is an important entity of the liquid phase chemistry.^{1–7} Despite its importance, our understanding of the factors that determine Λ_0 is still poor. The complexity of the problem drew the attention of great scientists like Born, Debye, and Onsager, but even then many of the basic aspects of the problem are not yet well-understood. The reason for the lack of progress is many fold. Not only are the interactions involved long-ranged but also the structure and the dynamics of the solvents involved are complex and were *hitherto* largely unknown. For example, it has been discovered only recently that water, acetonitrile, and methanol—all possess an *ultrafast* polar solvent response in 50–100 fs time scale.^{8,9}

Clearly, this ultrafast response will have an important effect on ionic conductance as well.

In this article, we are concerned with the limiting ionic conductance (Λ_0) in aqueous solution only. The value of the limiting ionic conductance, Λ_0 , is determined by the interaction between the ion and the solvent molecules and the relative dynamics of the solute–solvent system. Λ_0 itself shows several interesting, even anomalous, behaviors which are nontrivial to explain. In the following we list some of these.

1. The limiting ionic conductance, Λ_0 , shows a maximum when plotted against the inverse of the crystallographic ionic radius, r_{ion}^{-1} . This particular feature is shown in Figure 1 which also depicts the complete breakdown of Stokes' law for small ions like Li^+ and Na^+ .

2. Λ_0 shows a strong temperature dependence. For monovalent simple ions (for example, tetraalkylammonium ions and alkali metal ions), the temperature coefficient of Λ_0 is almost 2% per degree².

3. Λ_0 exhibits a significant solvent isotope effect. Experimental results reveal that Λ_0 of a particular ion in D_2O is 20% less than that in H_2O . This reduction of mobility is universal for all monopositive ions irrespective of their size.

None of the above results can be explained in terms of the Stokes–Einstein relation which relates the diffusion coefficient (or the conductivity) of the ion to the viscosity (η_0) of the medium. Traditionally, there have been two general approaches to rationalize the breakdown of Stokes' law. The phenomenological solvent-berg model² assumes the formation of a rigid solvent cage around a small ion which leads to an increase of the effective radius of the ion. This, in turn, leads to a sharp decrease of the conductivity (see Figure 1). In addition, the maximum in Λ_0 near Cs^+ is explained in terms of the

[‡] Electronic mail address: bbagchi@sscu.iisc.ernet.in. Also at the Jawaharlal Nehru Center for Advanced Scientific Research, Jakkur, Bangalore.

[⊗] Abstract published in *Advance ACS Abstracts*, June 1, 1997.

(1) Glasstone, S. *An Introduction to Electrochemistry*; Litton Education Publishing: New York, 1942. Bockris, J. O'M.; Reddy, A. K. N. *Modern Electrochemistry*; Plenum: New York, 1973.

(2) Atkins, P. W. *Physical Chemistry*, 5th ed.; Oxford University Press: 1994; Part III, Chapter 24. Castellan, G. W. *Physical Chemistry*, 3rd ed.; Addison-Wesley: Reading, MA, 1971; Chapter 31. Harned, H. S.; Owen, B. B. *The Physical Chemistry of Electrolyte Solutions*, 3rd ed.; Reinhold: New York, 1958.

(3) Frank, H. S. *Chemical Physics of Ionic Solutions*; Wiley: New York, 1956. Robinson, R. A.; Stokes, R. H. *Electrolyte Solutions*, 2nd ed.; Butterworth: London, 1959. Kay, R. L. In *Water, A Comprehensive Treatise*; Franks, F., Ed.; Plenum: New York, 1973; Vol. 3.

(4) Sadek, H.; Fuoss, R. M. *J. Am. Chem. Soc.* **1954**, *76*, 5902.

(5) Graham, J. R.; Gordon, A. R. *J. Am. Chem. Soc.* **1957**, *79*, 2350. Graham, J. R.; Kell, G. S.; Gordon, A. R. *J. Am. Chem. Soc.* **1957**, *79*, 2352.

(6) Gover, T. A.; Sears, P. G. *J. Am. Chem. Soc.* **1956**, *60*, 330.

(7) Daggatt, H. M.; Bair, E. J.; Kraus, C. A. *J. Am. Chem. Soc.* **1951**, *73*, 799.

(8) Jimenez, R. et al. *Nature* **1994**, *369*, 471. Rosenthal, S. J. et al. *J. Chem. Phys.* **1991**, *95*, 4715. Horng, M. L.; Gardecki, J. A.; Papazyan, A.; Maroncelli, M. *J. Phys. Chem.* **1995**, *99*, 17311. Bingemann, D.; Ernsting, N. P. *J. Chem. Phys.* **1995**, *102*, 2691.

(9) (a) Roy, S.; Bagchi, B. *J. Chem. Phys.* **1993**, *99*, 1310. (b) Biswas, R.; Bagchi, B. *J. Phys. Chem.* **1996**, *100*, 4261. (c) Nandi, N.; Roy, S.; Bagchi, B. *J. Chem. Phys.* **1995**, *102*, 1390. (d) Biswas, R.; Nandi, N.; Bagchi, B. *J. Phys. Chem. B* **1997**, *101*, 2968.

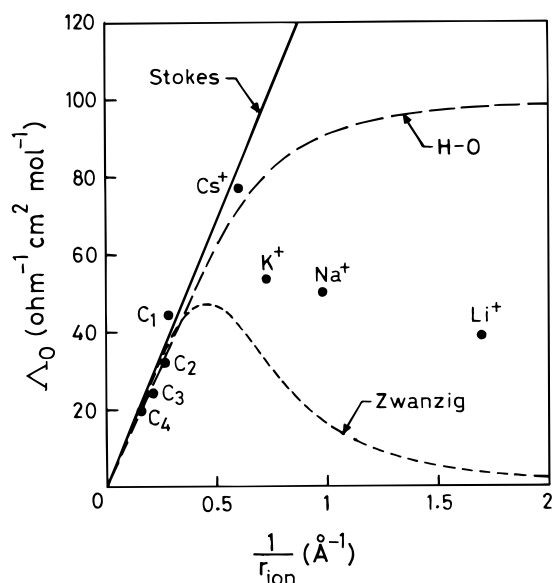


Figure 1. The values of the *Limiting ionic conductivity* (Λ_0) of rigid, monovalent ions in water (H_2O) at 298 K are plotted as a function of the inverse of the crystallographic ionic radius, r_{ion}^{-1} . The experimental results are denoted by the solid circles. The solid line represents the predictions of the Stokes' law, the large-dashed line the Hubbard-Onsager theory, and the small dashed line the theory of Zwanzig (with slip boundary condition). Note that the Stokes' law is valid for tetraalkylammonium ions C_1 – C_4 where $C_n = (\text{C}_n\text{H}_{2n+1})_4\text{N}^+$, n being 1, 2, 3 or 4.

orientational *structure breaking* of the solvent by the ion.¹⁰ However, this approach fails completely to provide a coherent quantitative description of Λ_0 . The second approach was initiated by Born¹¹ who suggested that because of the increased dissipation of momentum due to the long range ion-solvent interactions, the ion experiences an additional friction over and above the prediction of Stokes' law. The friction acting on the moving ion can, therefore, be written as a sum of two contributions

$$\zeta = \zeta_{\text{bare}} + \zeta_{\text{DF}} \quad (1)$$

where ζ_{bare} is the friction due to short range nonpolar interactions, whereas ζ_{DF} is the dielectric friction originating from the long-range polar interactions. Conventionally, ζ_{bare} is approximated by the Stokes' relation with a proper boundary condition. The main emphasis of this approach is the calculation of the dielectric friction, ζ_{DF} . This is, of course, nontrivial. Initially, ζ_{DF} was obtained by continuum models, but more recently a microscopic approach has been initiated.^{12,13} In the following we first briefly describe the main results of the continuum models.

The first consistent electrohydrodynamic calculation of dielectric friction was presented by Zwanzig.¹⁴ It leads to a simple expression for ζ_{DF} in terms of the static dielectric constant (ϵ_0) and the Debye relaxation time (τ_D). The resulting expression can explain the nonmonotonic size dependence of Λ_0 but

overestimates the dielectric friction by a factor of 3–5 for small ions like Na^+ and Li^+ . This is shown in Figure 1. In a different continuum approach,^{15,16} Hubbard and Onsager (H-O) derived an expression for the total friction acting on the ion by generalizing the Navier-Stokes equations for hydrodynamic flow to include the polarization relaxation of the solvent in the vicinity of the moving ion. The resulting hydrodynamic equations were then solved with the constraint of invariance of the energy dissipation with respect to rigid body kinematic transformation (rotation and translation). The Hubbard-Onsager continuum electrohydrodynamic approach constitutes a beautiful treatment of macrodynamics, and it predicts the mobility of large ions correctly. However, it severely underestimates the value of ζ_{DF} and thus fails to provide a quantitative description of the ion transport mechanism. This is also shown in Figure 1.

In a complete breakaway from the continuum models, Wolynes proposed a theory to obtain the dielectric friction, ζ_{DF} , from the force-force time correlation function—the force on the ion was obtained from microscopic quantities, such as the radial distribution function.¹² The theory was found to be rather successful in describing many aspects of the ionic mobilities in water and acetonitrile.^{12c} Several limitations of this approach were removed in a subsequent theory which pays proper attention to the various static and dynamic aspects of the ion-solvent composite system.^{17,18} A notable feature of the extended theory is the self-consistent treatment of the self-motion of the ion and the biphasic polar solvent response. The results were found to be in satisfactory agreement with all the known results not only for water and acetonitrile¹⁷ but also for monohydroxy alcohols.¹⁸ Most notably, the nonmonotonic dependence of Λ_0 on r_{ion}^{-1} was correctly reproduced for all these solvents. However, no theoretical studies on temperature dependence or solvent isotope effect on limiting ionic conductivity has been carried out. As already mentioned, the recently discovered ultrafast component in solvation dynamics is expected to play an important role in determining the solvent isotope effect and the temperature and pressure dependencies of Λ_0 .

Nevertheless, the strong temperature dependence of Λ_0 in water is certainly paradoxical. On increasing the temperature from 283 to 318 K, the density of water decreases by only about 1%, the static dielectric constant by about 15%, and the Debye relaxation time τ_D and the solvent viscosity both by about 50%.¹⁹ On the other hand, Λ_0 for Li^+ increases by 120%, from 26.37 at 283 K to 58.02 at 318 K. The same trend of increase is observed not only for Cs^+ , Na^+ , and Li^+ but also for the relatively large tetraalkylammonium ions.¹⁰ As this large change cannot be easily accounted for within the existing continuum model theories, explanations were offered in the past by invoking the partial breakdown of the hydrogen bonded network at high temperatures and formation of solvent-berg at low temperatures.¹⁰ Not only that such pictures are difficult (if not impossible) to quantify, but there is no experimental evidence of significant structural change between, for example, 283 and 298 K where Λ_0 changes by about 50%. Thus, explanation of the temperature coefficient of Λ_0 has remained largely unsolved.

In contrast to the temperature dependence, the solvent isotope effect on limiting ionic conductivity is less anomalous.¹⁰ For Na^+ , the change in Λ_0 is about 20% when the solvent is changed from H_2O to D_2O . This is comparable to the viscosity change of the liquid and, in principle, could be explained by

(10) (a) Kay, R. L.; Evans, D. F. *J. Phys. Chem.* **1966**, *70*, 2325. (b) Ueno, M. et al. *J. Chem. Phys.* **1996**, *105*, 3662.

(11) Born, M. *Z. Phys.* **1920**, *1*, 221.

(12) (a) Wolynes, P. G. *Ann. Rev. Phys. Chem.* **1980**, *31*, 345. (b) Wolynes, P. G. *J. Chem. Phys.* **1980**, *68*, 473. (c) Colonomos, P.; Wolynes, P. G. *J. Chem. Phys.* **1979**, *71*, 2644.

(13) Bagchi, B. *J. Chem. Phys.* **1991**, *95*, 467.

(14) Zwanzig, R. *J. Chem. Phys.* **1963**, *38*, 1603; **1970**, *52*, 3625.

(15) Hubbard, J. B.; Onsager, L. *J. Chem. Phys.* **1977**, *67*, 4850.

(16) Hubbard, J. B. **1978**, *68*, 1649. Hubbard, J. B.; Wolynes, P. G. In *The Chemical Physics of Solvation*; part C Dogonadze, R. et al., Eds.; Elsevier: New York, 1988; Chapter 1, p 33.

(17) Biswas, R.; Roy, S.; Bagchi, B. *Phys. Rev. Lett.* **1995**, *75*, 1098.

(18) Biswas, R.; Bagchi, B. *J. Chem. Phys.* **1997**, *106*, 5587.

(19) *CRC Handbook of Chemistry and Physics*, 57th ed.; Weast, CRC Press: 1976–1977.

hydrodynamics—via the continuum models—except that they all give a completely wrong magnitude of Λ_0 .

The molecular theory presented here describes the ion transport in terms of the ion–solvent interaction, the solute-modified solvent-structure around the ion, the orientational solvent static correlations, and the inherent dynamics of the medium. The effect of the motion of the ion on its own conductivity has also been taken into account through a self-consistent calculation. The present microscopic theory is shown to provide a good description for both the temperature dependence of Λ_0 and the solvent isotope effects on limiting ionic conductivity. The strong temperature dependence is seen to arise from a collection of several small microscopic effects, all acting in the same direction in a concerted fashion. These effects include a change in the ion-dipole direct pair correlation function and in the dynamics of the solvent. The theory also provides a fairly satisfactory description of the solvent isotope effect.

The organization of the rest of the paper is as follows. In the next section we briefly describe the molecular theory. In section III we present the calculational details of the ion-dipole direct correlation function. The same for the other necessary quantities is given in the Appendix II. We present numerical results of the temperature dependence of the limiting ionic conductivity in the section IV. Section V contains the results on the solvent isotope effect. We conclude the paper with a brief discussion in section VI.

II. The Molecular Theory

The microscopic theory presented here is based on the following simple picture. As an ion moves in the liquid, it experiences fluctuating forces from two different sources. First, there is the usual force from the short range, primarily repulsive, non-polar interaction with the surrounding solvent molecules. The friction originating from this part, as already mentioned, is termed as bare friction (ζ_{bare}). This is calculated from the solvent viscosity (η_0) and the crystallographic radius of the ion, (r_{ion}) by using the Stokes' law as follows $\zeta_{\text{bare}} = 4\pi\eta_0 r_{\text{ion}}$. This is clearly an approximation since the hydrodynamics cannot be valid for a ion which is smaller in size than the solvent. However, for small ions ζ_{bare} is generally much smaller than ζ_{DF} , and, therefore, the error made is not significant.¹² The second part of the fluctuating force originates from the long-range ion-dipole interaction. This gives rise to the dielectric friction, ζ_{DF} . We neglect the cross correlations among the short range, repulsive and long range attractive ion-dipole interactions. This is also an approximation first proposed by Wolynes¹² and used extensively in their subsequent works.¹² Due to the long range nature of the ion-dipole interaction, this polar force can be obtained from the well-known time dependent density functional theory.^{12,13} The latter provides an expression of the effective potential on the ion in terms of the fluctuating space and orientation dependent density—this expression is given in the Appendix I. The force due to the polar interaction is obtained from this potential. It should be stressed here that the present approach has been enormously successful in many areas of liquid state dynamics,^{20–22} and is an effective way to treat the dynamics of a strongly correlated system like the present one.

Table 1. Solvent Static Parameters at Three Different Temperatures

solvent	temp (K)	diameter (Å)	μ (D)	ρ (gm/cc)	η_0 (cp)
H ₂ O	283	2.8	1.850	0.9997	1.3070
H ₂ O	298	2.8	1.850	0.9970	0.8904
H ₂ O	318	2.8	1.850	0.9902	0.5960
D ₂ O	298	2.8	1.855	1.1045	1.0970

The dielectric friction, ζ_{DF} , is now calculated from the force–force time correlation function using Kirkwood's formula²³ which in the present case is given by

$$\zeta_{\text{DF}} = \frac{1}{3k_{\text{B}}T} \int_0^{\infty} dt \langle \mathbf{F}_{\text{id}}(0) \cdot \mathbf{F}_{\text{id}}(t) \rangle \quad (2)$$

where $\mathbf{F}_{\text{id}}(t)$ is the force acting on the ion due to the ion-dipole interaction only. As usual, k_{B} is the Boltzmann constant and T is the temperature in degree Kelvin. $\langle \dots \rangle$ stands for the ensemble averaging. The final expression for ζ_{DF} is given by¹⁷

$$\zeta_{\text{DF}}(z) = \frac{2k_{\text{B}}T\rho_0}{3(2\pi)^2} \int_0^{\infty} dt e^{-zt} \int_0^{\infty} dk k^4 |c_{\text{id}}^{10}(k)|^2 S_{\text{ion}}(k,t) S_{\text{solvent}}^{10}(k,t) \quad (3)$$

where $c_{\text{id}}^{10}(k)$ is the Fourier transform of the longitudinal component of the static ion-dipole direct correlation function. $S_{\text{solvent}}^{10}(k,t)$ is the longitudinal component of the *orientational* dynamic structure factor of the pure solvent with k as the wave-vector conjugate to the distance vector \mathbf{r} . While $c_{\text{id}}(k)$ describes the effective interaction between the ion and the dipolar solvent molecules, $S_{\text{solvent}}^{10}(k,t)$ describes the pure solvent dynamics. In defining these correlation functions, the wavenumber k is taken parallel to the z axis. ρ_0 is the average number density of the solvent. $S_{\text{ion}}(k,t)$ denotes the self dynamic structure factor of the ion. The $z = 0$ limit of eq 3 provides the macroscopic friction. The details are available in refs 17 and 18—a brief summary of derivation of eq 3 is given in the Appendix I for the sake of completion.

Equation 3 is a nonlinear, microscopic expression for the dielectric friction. It is nonlinear since it involves $\zeta_{\text{DF}}(z)$ on both the sides. Thus, it has to be solved self-consistently. This equation has an interesting structure as it couples single particle motion ($S_{\text{ion}}(k,t)$) to the collective dynamics of the solvent ($S_{\text{solvent}}(k,t)$) via the ion-dipole direct correlation function ($c_{\text{id}}(k)$). To obtain ζ_{DF} ($\equiv \zeta_{\text{DF}}(z=0)$) from eq 3, we need to specify both $S_{\text{solvent}}^{10}(k,t)$ and $S_{\text{ion}}(k,t)$. The latter is assumed to be given by

$$S_{\text{ion}}(k,t) = \exp[-D_T^{\text{ion}} k^2 t] \quad (4)$$

where the diffusion coefficient of the ion, D_T^{ion} , itself is determined by the total friction ζ . As the motion of the ion occurs on a time scale larger than the dynamics of the dipolar solvent, eq 4 is sufficient for most purposes.

The determination of the orientational solvent dynamic structure factor is rather complex. It is determined by the static orientational structure, the frequency dependent dielectric function $\epsilon(z)$, and the translational and rotational diffusion coefficients, among others, of the dipolar liquid (here ordinary water and heavy water). The solvent static parameters and the dielectric relaxation data for both the liquids are summarized in Tables 1–3. The details of the methodology are available elsewhere,^{9,17,18} and we give a brief discussion on it in the Appendix II. Finally note that the expression for the dielectric

(20) Kirkpatrick, T. R.; Wolynes, P. G. *Phys. Rev. A* **1987**, *35*, 3072.

(21) Kirkpatrick, T. R. *Phys. Rev. A* **1985**, *32*, 3130. Kirkpatrick, T. R.; Nieuwoudt, J. C. *Phys. Rev. A* **1986**, *33*, 2651. Kirkpatrick, T. R. In *Proceedings of the International Conference on the Theory of the Structures of Noncrystalline Solids*; Alder, D., Eds.; Bloomfield Hills, MI, 1985.

(22) Hohenberg, P. C.; Halperin, B. I. *Rev. Mod. Phys.* **1977**, *49*, 435.

(23) Kirkwood, J. G. *J. Chem. Phys.* **1946**, *14*, 180.

Table 2

(a) The Dielectric Relaxation Parameters of H ₂ O ^a					
T (K)	ε ₁	τ ₁ (ps)	ε ₂	τ ₂ (ps)	ε ₃
283	83.83	12.145	6.18	1.498	4.49
298	78.3	8.32	6.18	1.02	4.49
318	71.51	5.538	6.18	0.683	4.49

(b) Frequency and Dielectric Constants for the High Frequency Librational Modes ^b						
n ₁ ²	Ω ₁ (cm ⁻¹)	n ₂ ²	Ω ₂ (cm ⁻¹)	n ₃ ²	Ω ₃ (cm ⁻¹)	n ₄ ²
4.49	69.3	4.2	193	2.1	685	1.77

^a These data are well compiled in ref 9c. [$\epsilon_1 = \epsilon_0$, the static dielectric constant of the solvent; $\epsilon_3 = \epsilon_\infty$, the infinite frequency dielectric constant obtained by fitting the low frequency relaxation to a sum of two Debye dispersions]. ^b We have used the same high frequency dielectric dispersion data and low frequency dispersions for all the three different temperatures except the temperature dependent ϵ_0 .

Table 3

(a) Dielectric Relaxation Parameters of D ₂ O ^a							
solvent	ε ₁	τ ₁ (ps)	ε ₂				
D ₂ O	78.3	10.37	4.8				

(b) Frequency and Dielectric Constants for the High Frequency Librational Modes							
solvent	n ₁ ²	Ω ₁ (cm ⁻¹)	n ₂ ²	Ω ₂ (cm ⁻¹)	n ₃ ²	Ω ₃ (cm ⁻¹)	n ₄ ²
D ₂ O	4.8	64.0	4.2	184	2.1	505	1.77

^a These data are also well compiled in ref 9c. ^b $n_1^2 = \epsilon_\infty$, $n_4^2 = n^2$, the optical dielectric constant of the solvent.

friction (eq 3) has essentially the same structure as the solvation energy time correlation function ($S(t)$) except that the former (eq 3) has a *quartic* wavenumber (k) dependence, while that of the latter has a *quadratic* k dependence. Thus, the present theory can be considered as a dynamic solvent berg model.¹⁸

III. Determination of the Intermolecular Coupling between the Solute Ion and the Dipolar Solvent Molecules, $c_{id}(k)$

In this section, we describe the calculation of the wavenumber (k) dependent ion-dipole direct correlation function, $c_{id}(k)$, which describes the coupling of the solute ion with the distorted solvent structure around the ion.

We obtain the ion-dipole direct correlation function, $c_{id}(k)$, by Fourier transforming the expression of microscopic polarization ($P_{mic}(r)$) given by Chan et al.²⁴ An interesting aspect of this expression is that it predicts a region of negative values of $P_{mic}(r)$ which indicates the alignment of the solvent dipole just outside the first solvation shell in a direction opposite to that of those as the nearest neighbors.²⁴ The expression for the ratio of the microscopic polarization, $P_{mic}(r)$ to the macroscopic polarization, $P_{mac}(r)$ is given as follows²⁴

$$\frac{P_{mic}(r)}{P_{mac}(r)} = 1 - r \times \frac{dF(r)}{dr} + F(r) \quad (5)$$

where $F(r)$ is a dimensionless quantity and appears as a correction factor to the macroscopic polarization—the latter is given by the following expression²⁴

$$P_{mac}(r) = \frac{(\epsilon_0 - 1)ze}{4\pi\epsilon_0 r^2} \quad (6)$$

where e denotes the electronic charge and z the valency of the ion. We have calculated $P_{mic}(r)/P_{mac}(r)$ using the two mutually exclusive conditions given in the paper by Chan et al.²⁴ In Figure 2 we show the calculated variation of the polarization ratio with r (scaled by solvent diameter) in water for solute–solvent size ratio, 1. It is clear from the above figure (Figure 2) that the polarization density around an ion is oscillatory in nature which is maximum at the contact. This is in contrast to the dielectric saturation theory which predicts a divergence in the local static dielectric constant and thus in the local polarization near the ion.

IV. Numerical Results for Λ_0 in Water: Temperature Dependence

In this section we present the numerical results on the temperature dependent limiting ionic conductivity, Λ_0 . We calculate Λ_0 by using the following well-known *Nernst–Einstein* relation

$$\Lambda_0 = \frac{z^2 F^2 D_T^{\text{ion}}}{RT} \quad (7)$$

where F is the amount of electricity transported by one gram-equivalent of the conducting ion, and R is the universal gas constant. D_T^{ion} is the translational diffusion coefficient of the ion and is calculated from the Einstein relation

$$D_T^{\text{ion}} = \frac{k_B T}{\zeta} \quad (8)$$

where the total friction ζ is evaluated from eq 1. Note that no adjustable parameter is used at any stage of the calculation.

The calculated limiting ionic conductivity at 283 K is shown in Figure 3 where Λ_0 is plotted as a function of the inverse of the crystallographic ionic radius, r_{ion}^{-1} . The available experimental results¹⁰ are also shown in the same figure (Figure 3). The comparison clearly indicates a fair agreement between the theoretical predictions and the experimental results. In particular, the nonmonotonic size dependence is correctly reproduced by the present molecular theory. This is indeed satisfactory if one considers the complex nature of the solvent and the approximations involved. There are, however, still some minor discrepancies. The theory predicts a peak value for Λ_0 which is smaller than the experimental value by about 10%. Moreover, the theory predicts a shift in the peak position where the theoretical peak in Λ_0 corresponds to K^+ , while that in the experiment is for Cs^+ . For Li^+ , the calculated Λ_0 is about 15% greater than that of the experimental results.

In Figure 4 we present the calculated limiting ionic conductivity, for water at 298 K. The relevant experimental results¹⁰ are again shown in the same figure (Figure 4). The agreement here is excellent. In Figure 5 we compare the theoretical predictions on limiting ionic conductivity with those from the experiments by plotting Λ_0 against r_{ion}^{-1} at 318 K. The relevant experimental results¹⁰ are also shown in the same figure (Figure 5). Note that the theory predicts the peak value of Λ_0 quite successfully but again fails to describe the experimental results for Na^+ and Li^+ quantitatively.

The fair agreement between the theoretical predictions and the experimental results indicates that the present theory can capture essentially all the static and dynamic aspects of the solute-solvent system correctly at different temperatures. We

(24) Chan, D. Y. C.; Mitchel, D. J.; Ninham, B. W. *J. Chem. Phys.* **1979**, *70*, 2946.

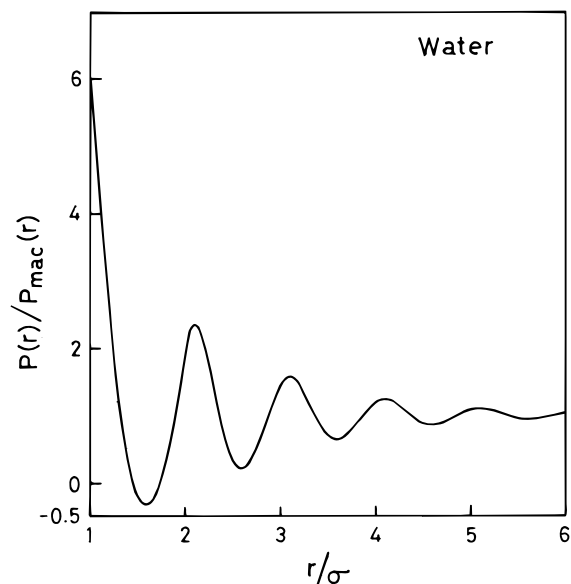


Figure 2. The ratio of the solvent microscopic polarization to the macroscopic polarization, $P_{\text{mic}}(r)/P_{\text{mac}}(r)$ is plotted as a function of r , for water (H_2O) at 298 K. The solute–solvent size ratio is 1. Note that r is scaled by the solvent diameter, σ .

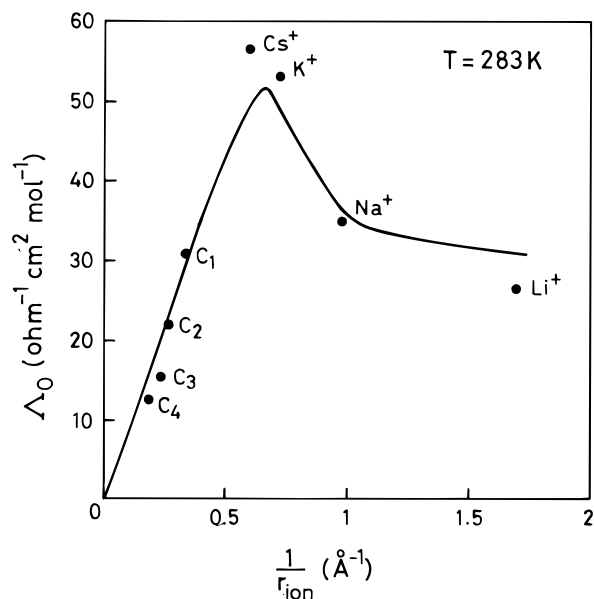


Figure 3. The values of the limiting ionic conductivity (Λ_0) of rigid, monovalent ions are plotted as a function of the inverse ionic radius, r_{ion}^{-1} in water (H_2O) at 283 K. The solid line represents the predictions of the present microscopic theory. The solid circles denote the experimental results.

would like to emphasize again that this agreement has been achieved without the use of any adjustable parameter.

The reasons for the remaining discrepancies are not clear. It is likely that the MSA model used to obtain the static pair correlations does not describe the real solvent accurately. Another reason may be the use of the dielectric relaxation data which at 283 and at 318 K were obtained from those at 298 K by scaling the relaxation times linearly with the viscosity. Any slight incompatibility in these data will be magnified in the calculation of Λ_0 . This is more so for the relatively small ions because the small ion couples with the dynamic response of the solvent more strongly compared to the larger ions.

Let us now comment on the physical origin of the strong temperature dependence of Λ_0 . The present theory takes into account the temperature effect through various molecular

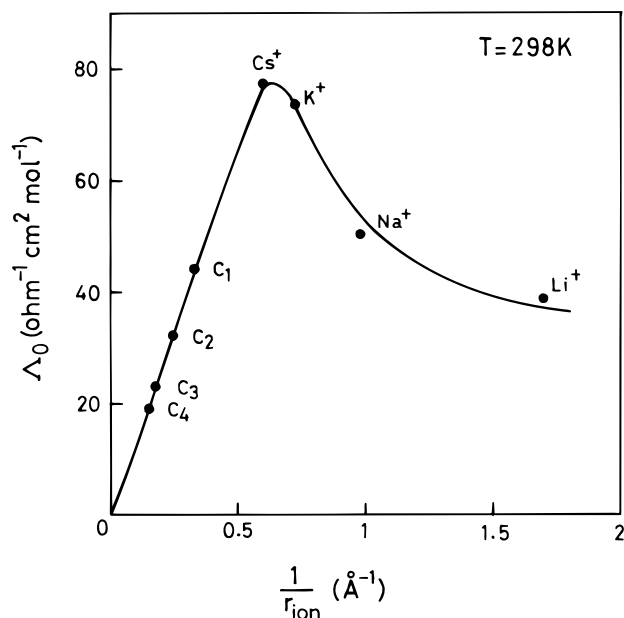


Figure 4. The values of the limiting ionic conductivity (Λ_0) are plotted as a function of the inverse crystallographic ionic radius, r_{ion}^{-1} in water (H_2O) at 298 K. The representations remain the same as Figure 3.

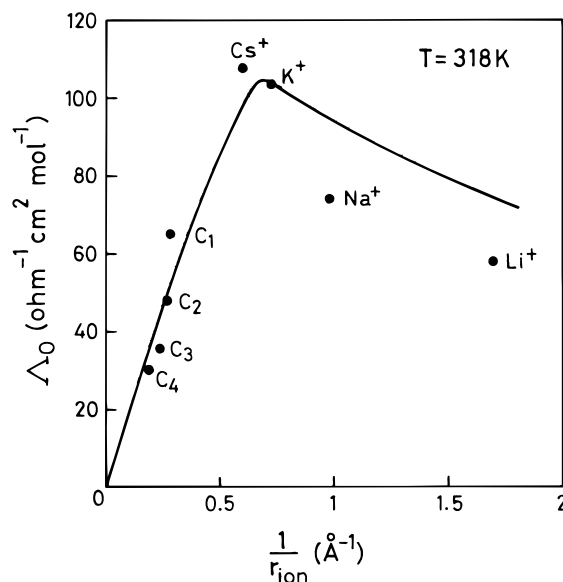


Figure 5. The values of the limiting ionic conductivity (Λ_0) of rigid, monovalent ions are plotted as a function of the inverse crystallographic ionic radius in water (H_2O) at 318 K. The solid line represents the predictions of the present theory, and the solid circles denote the experimental results.

parameters, each contributing a small effect with the change in the temperature. These effects act in a concerted fashion to a single direction—either to decrease or increase the limiting ionic conductivity depending upon the direction in which the temperature is changed. For example, the increase in the temperature from 283 to 318 K gives a $\sim 10\%$ reduction in the polarity (3Y) parameter. This translates into the similar reduction in the orientational static correlations and ion-dipole direct correlation functions. The viscosity of the solvent also reduced by $\sim 50\%$. This reduction in the solvent viscosity changes Λ_0 in two ways—changing both the bare friction and the dielectric friction. The reduced viscosity also decreases the Debye relaxation times which have been used to evaluate the dynamic solvent structure factor, $S_{\text{solvent}}^{10}(k, z)$ through the calculation of $\Sigma(k, z)$. In order to understand the dynamics of solvent response,

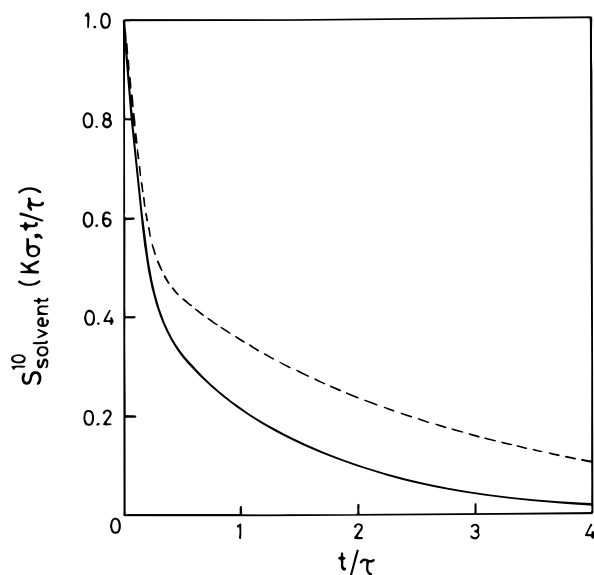


Figure 6. The rate of the decay of the orientational, dynamic solvent structure factor, $S_{\text{solvent}}^{10}(k\sigma, t/\tau)$ as a function of time, t , for water at two different temperatures. The solid and the dashed lines represent the decay of $S_{\text{solvent}}^{10}(k, t)$ at 318 and 283 K, respectively. Note that the numerical results obtained with $k\sigma = 6.3$ where σ is the diameter of a water molecule. The wavenumber (k) and the time (t) are scaled by the solvent diameter (σ) and the time τ , respectively. The parameters used for this calculation are given in Tables 1 and 2. $\tau = 1 \times 10^{-12}$ s.

we plot in Figure 6 the calculated dynamic solvent structure factor (normalized), $S_{\text{solvent}}^{10}(k, t)$, for two different temperatures. Note $S_{\text{solvent}}^{10}(k, t)$ is obtained by numerically Laplace inverting $S_{\text{solvent}}^{10}(k, z)$, and we show the results for intermediate wave-number only. It is clear from the above figure that the response function at high temperature decays more rapidly than that at the low temperature. This, in turn, produces less dielectric friction at the high temperature.

It is interesting to see how so many changes act in the same direction. Thus, we are in a position now to understand the anomalous temperature coefficient of the limiting ionic conductance in aqueous electrolyte solutions.

V. Numerical Results for Λ_0 in Heavy Water D_2O : Solvent Isotope Effect

Here we present the theoretical results on ionic conductivity in heavy water (D_2O) at 298 K. The necessary static parameters and dielectric relaxation data needed for the calculation of Λ_0 in D_2O are given in Tables 1 and 3.

The calculated results for the limiting ionic conductivity, Λ_0 , in heavy water (D_2O) at 298 K are shown in Figure 7. The available experimental results¹⁰ for D_2O are also shown in the same figure (Figure 7). The theoretical results are seen to be again in good agreement with those from the experimental ones. Note that the theory can successfully predict the peak value of Λ_0 in D_2O . The experimental observation that the solvent isotope effect reduces the mobility by about 20% is correctly reproduced here.

In view of the present isotope effect, it is interesting to recall the significant isotope effect observed in electron mobility.²⁵ The latter is, of course, a more difficult problem as a fully quantum mechanical treatment is required to understand the nature of the solvent isotope effect on electron mobility.²⁵

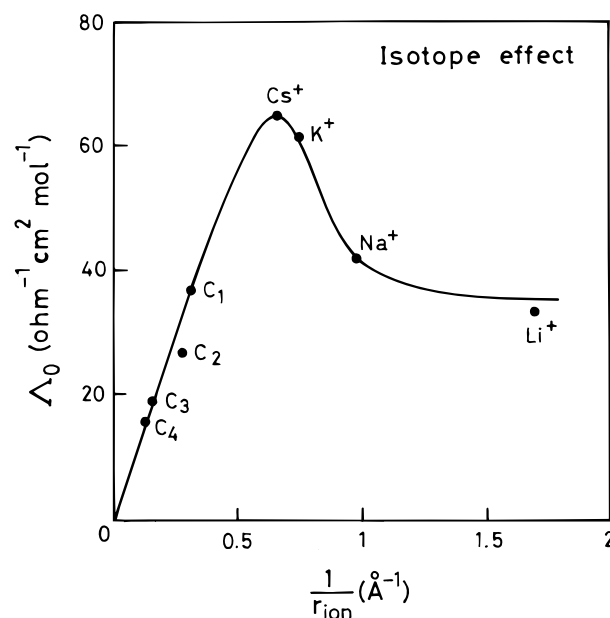


Figure 7. The effect of isotopic substitution in solvent on limiting ionic conductivity in electrolyte solution. The values of the limiting ionic conductivity, Λ_0 are plotted as a function of the inverse of the crystallographic ionic radius in heavy water (D_2O) at 298 K. The prediction of the present molecular theory is represented by the solid line while those from experiments are shown by the solid circles.

VI. Conclusion

Let us first summarize the main results of this paper. We have presented a microscopic calculation which explains the anomalous temperature dependence of the limiting conductivity of unipositive ions in aqueous solutions. The strong temperature dependence is shown to arise from a collection of small effects all acting in the same direction. Thus, one need not invoke any unquantifiable physical concepts like the formation or breaking of solvent-berg to explain the experimental results. The theory can also explain the significant solvent isotope effect which has been known for a long time but was not *hitherto* explained quantitatively. The nonmonotonic size dependence of limiting ionic conductivity at various temperature has also been correctly described in terms of the dielectric friction.

An important aspect of the present study is the systematic incorporation of the ultrafast polar solvent response in calculating the ionic mobilities at all temperatures reported here. In a microscopic theory of polar solvation dynamics developed earlier⁹ it has been shown that in the theory the ultrafast polar solvent response comes entirely from the dynamic response function $\Sigma(k, z)$ which is determined in turn by the fast components dielectric dispersion of the pure solvent. We use the same $\Sigma(k, z)$ in the present theory to calculate the limiting ionic conductivities of various monopositive ions. An interesting prediction is that if we incorporate only the largest Debye relaxation time, then we find about 100% reduction of the value of the limiting ionic conductivity obtained using the full dielectric relaxation data of the solvent.¹⁸

It is important to note that at room temperature the experimental results on limiting ionic conductivities of uninegative halide ions constitute a curve with a maximum which is different from that of the cations when plotted as a function of the crystallographic ionic radius. This indicates that the interaction between a solvent molecule and an anion is different and asymmetric from that of the cation-solvent system. Recent

(25) Schwartz, B. J.; Rossky, P. J. *J. Chem. Phys.* **1996**, *105*, 6997.

(26) Raineri, F. O.; Resat, H.; Friedman, H. L. *J. Chem. Phys.* **1992**, *96*, 3058.

(27) Lee, S. H.; Rasiaiah, J. C. *J. Chem. Phys.* **1994**, *101*, 6964. *J. Phys. Chem.* **1996**, *100*, 1420.

computer simulation studies by Lee and Rasaiah²⁷ (with improved interaction potential) have quantitatively reproduced the above experimental trend. The present theory, however, cannot explain the distinct maximum observed for the halide ions. This is because the present theory uses the ion–solvent direct correlation functions obtained from the MSA model which is *insensitive* to the sign of the charge. The present theory, in principle, can be extended to explain the differences by using the proper charge representation of the solvent molecules. That is, one needs to abandon the point dipole representation of the solvent molecules. While this is certainly worthwhile, the procedure would involve extensive numerical work.

The theory presented here is based on a simple idea, although its implementation requires the consideration of a rather large number of factors. One needs not only a detailed knowledge of the ion–dipole and dipole–dipole pair correlation functions of the solution but also a detailed description of the dielectric dispersion of the pure solvent. Even after these are obtained, one needs to calculate the rotational and the translational generalized frictions which are both frequency and wavenumber dependent. However, all the functions involved are well-behaved, and the self-consistent calculation of ζ_{DF} is straightforward. In fact, given the complexity of the problem, it is difficult to imagine that a simpler theory than the present one can be successful.

We now comment on the validity of the separation of the total friction into two parts—namely, the bare friction (ζ_0) and the dielectric friction (ζ_{DF}). This separation may not be a serious approximation. It has been discussed earlier¹³ that so long as the bare (nonpolar) part contains only the isotropic part of the interaction potential between the ion and the solvent dipoles, such a separation is internally consistent within the linearized equilibrium theory of liquids. This has also been observed in the simulation studies of Berkowitz and Wan.²⁸ However, this separation becomes questionable if nonlinear effects are important, as discussed in ref 13.

The theory presented here can be extended to understand the concentration dependence of ionic conductivity in electrolytes of rigid ions like NaCl. Work in this direction is under progress.

Acknowledgment. The work reported here has been supported in part by grants from the Council of Scientific and Industrial Research (CSIR) and the Department of Science and Technology (DST), India.

Appendix I

The force which is responsible for the dielectric friction is long range in nature since it originates from the coupling of the ionic field to the solvent polarization mode. The density functional theory provides the following expression for the force density on the ion

$$\mathbf{F}_{id}(\mathbf{r}, t) = k_B T n_{ion}(\mathbf{r}, t) \nabla \int d\mathbf{r}' d\mathbf{\Omega}' c_{id}(\mathbf{r}, \mathbf{r}', \mathbf{\Omega}') \delta\rho(\mathbf{r}', \mathbf{\Omega}', t) \quad (9)$$

where $n_{ion}(\mathbf{r}, t)$ is the number density of the ion, $\delta\rho(\mathbf{r}, \mathbf{\Omega}, t)$ is the fluctuation in the position (\mathbf{r}), orientation ($\mathbf{\Omega}$), and time (t) dependent number density (ρ_0) of the dipolar solvent, and $c_{id}(\mathbf{r}, \mathbf{r}', \mathbf{\Omega})$ is the ion–dipole direct pair correlation function (DCF). ∇ is the spatial gradient operator. Next, the density and the direct correlation function are expanded in the spherical harmonics. We then use the standard Gaussian decoupling approximation to obtain the microscopic expression for the frequency dependent dielectric friction, ζ_{DF} as given in eq 3. The same expression for the dielectric friction (eq 3) can also

be obtained from the mode coupling theory (MCT) which does not invoke Kirkwood's formula at any stage.^{29,30} Thus, exactly the same expression for friction can be derived by using these two alternate routes. Our understanding is that so long as one is calculating the friction, a properly defined random force gives the correct result.

Appendix II

The orientational solvent dynamic structure factor, $S_{solvent}^{10}(k, t)$ has the following form

$$S_{solvent}^{10}(k, t) = \frac{N}{4\pi 3Y} \left[1 - \frac{1}{\epsilon_L(k)} \right] \mathcal{L}^{-1} \left[z + \sum(k, z) \right]^{-1} \quad (10)$$

where \mathcal{L}^{-1} stands for Laplace inversion. $3Y$ is the polarity parameter of the solvent and can be calculated from dipole-moment μ and ρ_0 of the solvent using the following relation $3Y = (4\pi/3k_B T)\mu^2\rho_0$. N represents the total number of solvent molecules present in the system. $\epsilon_L(k)$ is the longitudinal (110) component of the wavenumber (k) dependent dielectric function. This is calculated from MSA corrected both at $k \rightarrow \infty$ and $k \rightarrow 0$ limits by using the XRISM results of Raineri, Resat, and Friedman.²⁶ $\sum(k, z)$ is the dynamic response function of the solvent which is a measure of the rate of orientational solvent polarization density relaxation and can be evaluated using the following expression

$$\sum(k, z) = \left[1 - \frac{\rho_0}{4\pi} c(110; k) \right] \left[\frac{2k_B T}{I[z + \Gamma_R(k, z)]} + \frac{k^2 k_B T}{m\sigma^2[z + \Gamma_T(k, z)]} \right] \quad (11)$$

where m , σ , and I characterize the mass, diameter, and the average moment of inertia of each solvent molecule, respectively. $c(110; k)$ is the (110) component of the two particle direct correlation function of the solvent in the wave-vector (\mathbf{k}) space. $\Gamma_R(k, z)$ and $\Gamma_T(k, z)$ are the rotational and the translational dissipative kernels, respectively, of the solvent. The calculation of the dynamic response function, $\sum(k, z)$ is a nontrivial exercise. It contains two friction kernels—the rotational kernel (Γ_R) and the translational kernel (Γ_T). The details regarding the former has been discussed in our earlier studies^{17,18} and here we give only the bare essentials.

(i) Rotational Friction, $\Gamma_R(k, z)$. We calculate the rotational friction, $\Gamma_R(k, z)$ by using directly the experimental results on dielectric relaxation and far infrared line shape measurements in water. The relation which connects $\Gamma_R(k, z)$ to the dielectric relaxation through the frequency dependent dielectric function, $\epsilon(z)$, is as follows

$$\frac{k_B T}{I[z + \Gamma_R(k = 0, z)]} = \frac{(\epsilon_0 - 1) z [\epsilon(z) - n^2]}{3Y n^2 (\epsilon_0 - \epsilon(z))} \quad (12)$$

where $3Y$ is the polarity parameter of the solvent with dipole-moment μ and is given as $3Y = (4\pi/3)\beta\mu^2\rho_0$, $\beta = (k_B T)^{-1}$. ϵ_0 and n^2 are static and optical dielectric constants of the solvent, respectively. In the present calculations, $\Gamma_R(k, z)$ for water has been obtained using the above relation in the following way. The frequency dependent dielectric function, $\epsilon(z)$ in the low frequency regime is described by two consecutive, well-separated Debye dispersions. The dielectric dispersions involved in Debye relaxations are given in Table 2a. At high frequency regime, $\epsilon(z)$ derives major contributions from the

(29) Balucani, U.; Zoppi, M. *Dynamics of the Liquid State*; Clarendon Press: Oxford, 1994; and references therein.

(30) Bhattacharyya, S.; Bagchi, B. *J. Chem. Phys.* **1997**, *106*, 1757.

(28) Berkowitz, M.; Wan, W. *J. Chem. Phys.* **1987**, *86*, 376.

librational and intermolecular vibrational motions of the hydrogen bonded network. These high frequency data are tabulated in Table 2b.

(ii) Solvent Translational Friction, $\Gamma_T(k,z)$. It has been found that the solvent translational motion can enhance the rate of solvation and the mobility of an ion by accelerating the rate of the solvent polarization relaxation. In the case of ionic mobility the most important and effective translational modes are those of nearest neighbor solvent molecules. Naturally, the solvent translational motion near the ion will be rather different

from those in the bulk since the strong ionic–dipole interaction quenches the free translational motion of the nearest neighbors. This is an example of the back reaction of the solute on the solvent which leads to an interesting dynamic cooperativity which is intrinsically nonlinear in nature. We have calculated the translational diffusion coefficient of the nearest neighbor solvent molecules through a nonlinear equation which couples the solvent translational mode with that of the ion.¹⁸

JA970118O